

Phosphoric acid activated carbon as borderline and soft metal ions scavenger

Md Mokhlesur Rahman, Siti Hadijah Samsuddin, Mohd Fuad Miskon, Kamaruzzaman Yunus & Alias Mohd Yusof

To cite this article: Md Mokhlesur Rahman, Siti Hadijah Samsuddin, Mohd Fuad Miskon, Kamaruzzaman Yunus & Alias Mohd Yusof (2015) Phosphoric acid activated carbon as borderline and soft metal ions scavenger, Green Chemistry Letters and Reviews, 8:2, 9-20, DOI: [10.1080/17518253.2015.1058974](https://doi.org/10.1080/17518253.2015.1058974)

To link to this article: <https://doi.org/10.1080/17518253.2015.1058974>



© 2015 The Author(s). Published by Taylor & Francis.



Published online: 04 Sep 2015.



Submit your article to this journal [↗](#)



Article views: 769



View related articles [↗](#)



View Crossmark data [↗](#)

Phosphoric acid activated carbon as borderline and soft metal ions scavenger

Md Mokhlesur Rahman^{a*}, Siti Hadijah Samsuddin^a, Mohd Fuad Miskon^b, Kamaruzzaman Yunus^b
and Alias Mohd Yusof^c

^aFaculty of Pharmacy, International Islamic University Malaysia, 25200 Kuantan, Pahang, Malaysia; ^bFaculty of Science, International Islamic University Malaysia, 25200 Kuantan, Pahang, Malaysia; ^cFaculty of Science, Universiti Teknologi Malaysia, 81310 Skudai, Johor, Malaysia

(Received 27 October 2013; final version received 12 May 2015)

Three activated carbons have been prepared, two from oil-palm shell and one from coconut shell, by the phosphoric acid activation process. Adsorption isotherms of copper(II) were determined to evaluate and compare the performance of experimental carbons. The obtained data are fitted very well to Langmuir and Freundlich adsorption models. All prepared activated carbons show 4–7-fold high adsorption capacity (q_{\max} 19.5–23/18.6–21 mg g⁻¹) than that of the commercial ones (q_{\max} 5.6/2.9 mg g⁻¹) under the conducted experimental conditions. The mechanism of adsorption was evaluated from the competitive adsorption of copper(II) and calcium(II) in a binary solution depending on their behaviour as Lewis acid and assessed as inner-sphere complexation. The competitive adsorption of copper(II) with other borderline and soft metal ions was evaluated by the best scavenger using a solution of ternary solute of copper(II), nickel(II) and lead(II). The adsorption selectivity order is determined as follows: Pb > Cu >> Ni.

Keywords: Activated carbon; chemical activation; adsorption; chemisorption; kinetics

1. Introduction

1.1. Background

The toxicity and threat of heavy metal species to human life and environment came into the limelight in the 1970s especially after the disclosure of mercury poisoning by the Minamata disaster in Japan (1). Since then, World Health Organization has set up various permissible limits on the discharge of heavy metals into the environment. The processing industries have increasingly been creating environmental problems generating heavy metals, of which the production of lead, copper and zinc had increased tremendously with a 10-fold increase by the years between 1850 and 1990 (2, 3). Heavy metals are also released from natural sources. Although various treatment processes are available in removing metal ions from aqueous solutions, activated carbon adsorption has advantages in selectivity and thermal and chemical stability (4). Activated carbons can be prepared in the laboratory from a large number of materials but the raw materials for commercial practice for active carbons are principally sawdust, coconut shells, black ash, charcoal, lignite, bituminous coal and petroleum coke (5). The residues from the carbonization and activation are found to have a large

pore volume and as this is derived from a very small diameter pores the internal surface area is high. This method produces an amorphous carbon that is not graphitized to any extent and it may not even be completely carbonized since charcoals contain rather high hydrogen content, approximately 5%. The surface area of active carbons may be extremely high, ranging from 450 to over 1500 m² g⁻¹, in the case of activated charcoals. The pore structure of activated charcoals can be quite well defined, and the pore distribution can be very narrow. For instance, in coconut charcoal almost the entire pore volume is in pores with diameters from 10 to 20 Å.

Many researchers found that the presence of ash content and inorganic matter in the starting materials was an important feature to avoid partial fusion and swelling in the carbonization stage. Therefore a new pre-treatment method had been established to remove the inorganic with diluted acidic solution before carbonization (6). Activated carbons are high-surface area, high porosity carbons that are produced by two principal methods: thermal activation and chemical activation. Thermal activation involves heating a previously charred material at high temperature in the presence of an oxidizing gas, such as CO₂,

*Corresponding author. Email: mdrahman@iium.edu.my

N₂, steam, and chemical activation involves heating a mixture of the raw material and a dehydrating agent to temperatures from 4000 to 10,000°C.(7) After carbonizing the dehydration agent is leached out and reused. The three dehydrating agents that are most commonly used are KOH, H₃PO₄ and ZnCl₂ (6–11). Huge amounts of oil palm and coconut shells are produced as agricultural wastes in Malaysia. The utilization of these shells as carbon precursor is very promising. Conventional activated carbons are effective in removing organic substances from water, but their use as metal ion scavenger is rare (WHO, Water Sanitation Health, (12)). It has been shown by many researchers (13, 14) that lignocellulosic agricultural wastes, particularly nutshells, are very good precursors for the removal of heavy metal ions from aqueous solutions. In this study, metal ion scavenger grade activated carbons were prepared from oil palm and coconut shells using low-temperature activation with phosphoric acid. In terms of impact, metal finishing practices, for example, electroplating, etching and preparation of metal components for numerous businesses, have been recognized as a main cause of wastes holding high concentrations of Pb and Ni (15), thus contributing to pollution problem in the particular area. Pb poisoning can cause reduced muscle coordination, nerve injury to the sense organs and nerves guiding the body, amplified blood pressure, reproductive problems and underdeveloped fatal growth even at low exposure levels. The most common harmful health effect of nickel in humans is an allergic skin reaction in particular for those who are sensitive to nickel (16). Ca availability is one of the major limiting factors affecting the distribution of many freshwater aquatic organisms in which they rely on calcium for their shell growth. Since Ca(II) is the most common and dominant ion present in natural water, the feasibility of any adsorbent to be used in drinking and wastewater treatment depends upon its preferential adsorption capacity of target ion over Ca(II).

The Ministry of Health, Malaysia, reported that from 1995 to 2012 there was an average of about 750 cases per year of pesticide and chemical poisoning (17, 18), where, the commonest poison used was a weed killer containing paraquat compound and insecticides containing organophosphates. In 1997, the Ministry of Health Malaysia introduced a surveillance programme for occupational and work-related diseases, including poisonings for cases seen in government health facilities. The programme notified 95 cases of poisoning by chemicals and pesticides and reported the commonest causes of occupational poisonings were paraquat (19%), organophosphates (16%), agro-chemicals excluding pesticides (15%) and

gases (10%). The mortality from paraquat poisoning is higher than that from any other type of poisoning associated with agricultural chemicals (19).

Paraquat is a potent, non-selective herbicide and potentially lethal when ingested (accidentally or intentionally). Pulmonary systems are mainly affected by paraquat poisoning. The gastrointestinal tract prevention of paraquat absorption is critical due to the limited means to significantly increase its elimination from the body (20). The fundamental treatment of paraquat poisoning is by means of gastrointestinal lavage and the selective excretion of toxic substances out of body following the administration of adsorbents. Clay minerals (21), cation exchange resin (22, 23), fuller's earth and bentonite used as adsorbents for the primary treatment of paraquat poisoning. Activated carbon, an adsorbent, is readily available and effective for the primary treatment of paraquat poisoning. Moreover, among adsorbents, activated carbon has been evaluated as a reliable, safe and inexpensive antidote and is recommended for use in the treatment of acute poisoning (24–26). *In vitro*, studies have shown that paraquat adsorbs onto activated carbon more rapidly and effectively in normal saline (0.9% sodium chloride solution) than in distilled water (27–29). Normal saline is the most suitable solvent for paraquat removal by activated carbon. These studies also showed the paraquat removal by activated carbon produced in ambient condition and commercially available activated carbon in distilled water and normal saline (0.9% NaCl) solution, respectively.

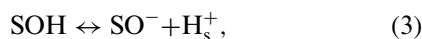
1.2. Adsorption equilibria

The nitrogen adsorption technique was used in determining the surface area and porosity development. Equilibrium parameters were determined from the batch adsorption experiment followed by fitting the data to various models. The adsorption performance was compared with that of a commercial activated carbon. The effect of pH and the co-presence of Ca (II) were tested to evaluate the feasibility and mechanism of adsorption. Since the basal structural units or graphitic layers of activated carbon are considered softer than the surface functional groups (30), the competitive effect of soft ion on the adsorption of borderline metal ion is very interesting. Adsorption of Cu(II), Ni(II) as borderline (31, 32) and Pb(II) as soft ion (32) was conducted from a multi-solute solution to determine the selectivity order. Langmuir and Freundlich adsorption isotherms (33) are widely employed to evaluate and compare the adsorption performance of adsorbents. According to the Gouy–Chapman–Stern–Grahame Model, the free energy of adsorption

can be defined, by Equation (1), as the sum of the free energy of the chemical interaction and that of an electrostatic force of attraction/repulsion (34, 35).

$$\Delta G_{\text{total}} = \Delta G_{\text{chemical}} + \Delta G_{\text{electrostatic}} \quad (1)$$

The pH of solution plays an important role in the adsorption of cations and anions, as described in the surface complex formation model (34, 36). According to this model, the surface functional groups of activated carbon can be modelled as a single, weak diprotic acid and can be represented by the following surface reactions (2) and (3). Since surface precipitation may occur at > pH 5 and since the pH_{ZPC} of the prepared carbon is circa 3, the initial pH of the experimental solution was varied, in this study, within 3–5 to ensure true and favourable adsorption (37).



where the symbol (SO^-) represents the active site of the surface and H_s^+ is the activity of the proton at the solid surface.

Following Langmuir Equation (4) is used to evaluate adsorption behaviour

$$q_e = \frac{q_{\text{max}} b C_e}{1 + b C_e}, \quad (4)$$

where q_e = amount of metal ion adsorbed at equilibrium per unit mass activated carbon (mg g^{-1}); C_e = equilibrium concentration of metal ion in solution (mg L^{-1}); q_{max} = the maximum monolayer adsorption capacity (mg g^{-1}) and b = affinity or adsorption constant, related to the heat of adsorption, ($\text{dm}^3 \text{g}^{-1}$).

The linear form of Equation (4) is derived as Equation (5) to determine the Langmuir parameters. Plotting C_e/q_e against C_e gives a straight line with a slope $1/q_{\text{max}}$ and an intercept $1/bq_{\text{max}}$.

$$\frac{C_e}{q_e} = \frac{1}{q_{\text{max}}} C_e + \frac{1}{b q_{\text{max}}}. \quad (5)$$

The Freundlich equation is expressed as

$$q_e = K_F C_e^{1/n}, \quad (6)$$

where q_e and C_e have the same meanings as in Equation (7), K_F and “ n ” are the Freundlich empirical constants that reveal the characteristic of adsorbent related to adsorption capacity and intensity, respectively.

The Freundlich constant, K_F unlike Langmuir constant, q_{max} does not predict the saturation of the solid surface by the monolayer coverage of the adsorbate (38). However, it gives a relative measure in adsorption capacity and estimates bond strength (13). The value of “ n ” discloses the adsorption pattern. The favourable adsorption is understood from the values of $1 < n < 10$ while irreversible adsorption is noticed from $n > 10$ and unfavourable from $n < 1$. The simplified linear logarithm form of Equation (6) is presented in Equation (7). Plotting $\log q_e$ against $\log C_e$ gives a straight line with a slope $1/n$ and an intercept $\log K_F$.

$$\log q_e = \log K_F + \frac{1}{n} \log C_e. \quad (7)$$

The effect of competing ion on the adsorption of a particular ion can be determined by the ratio of maximum monolayer adsorption capacities for the adsorption in the single- ($q_{\text{max-single}}$) and the multi-solute solution ($q_{\text{max-mix}}$), as described by the following Equations (8–10) (39):

$$\frac{q_{\text{max-mix}}}{q_{\text{max-single}}} > 1. \quad (8)$$

Indicating that the adsorption is promoted by the presence of other ions.

$$\frac{q_{\text{max-mix}}}{q_{\text{max-single}}} = 1. \quad (9)$$

There is no observable net interaction.

$$\frac{q_{\text{max-mix}}}{q_{\text{max-single}}} < 1. \quad (10)$$

2. Experimental design

2.1. Preparation

To enhance metal ion uptake capacity by concurrent activation/oxidation, acid pre-treated precursors were impregnated with H_3PO_4 acid and activated in a Carbolite muffle furnace. In this work, a 5% solution of H_2SO_4 was used in the pre-treatment to enhance surface acidity and porosity. In the previous work, H_3PO_4 concentration of 10–35% and pyrolysis temperature at 500°C was used for the highest development of pores (40). It can be seen that the smooth surfaces with many orderly pores were developed. Increasing the acid concentration accompanied the development of pores. This is due to the roles of impregnating agent that minimizes the formation of tars and other liquids, which could clog up the pores and inhibit the

development of pore structures. Pre-treatment was also explored with 30% H_3PO_4 (40). Acid pre-treatment controls volatile evolution in the activation of carbonaceous precursor (41). Guo and Lua (42) studied the effect of pre-treatment on oil-palm stones and showed that acidic groups were well developed from the samples pre-treated with 5% H_2SO_4 . The chamber of Carbolite muffle furnace is not air tight according to the product specification (Model: ELF 11/6B, Barloworld Scientific).

Commercial activated carbon (CAC), “Aktivkohle”, was obtained from Riedel-deHaën, Germany. Activated carbon preparation consists of raw material preparation and activation. Oil palm and coconut shells were collected from a local palm-oil processing factory and market places, respectively. The collected raw materials, oil palm and coconut shells, were washed, dried, crushed and sieved to the particle sizes of 1.18–2.36 mm. The crushing and grinding produced particles of the size range 1.18–2.36 mm. This size range was adequate for this research, since adsorption depends more on internal particle surface area than external surface area, which is controlled by particle diameter. Particle diameter is, however, important in determining the void space that exists between particles, and thus the pressure drop, in an adsorber bed. Further consideration of particle diameter would thus be important for actual use of these adsorbents in packed beds. After sieving, selected crushed particles were pre-treated by soaking in 5% H_2SO_4 for 24 h at room temperature (37°C) and this step is called pre-treatment. Finally the particles were washed with distilled water and dried. Prior to activation the prepared raw materials were impregnated with 30% aqueous H_3PO_4 , in a wt. ratio 1:1. The physical state of impregnated feedstock before charging in the furnace is termed as charge state. The activation was carried out at 500°C, with 2 h contact time in a muffled furnace. The products were thoroughly washed to about neutrality in a glass made Soxhlet’s apparatus. The removal of adhered phosphate was confirmed by adding a few drops of 30% solution of $\text{Pb}(\text{NO}_3)_2$ to the washings (43), then dried in an oven at 110°C and stored. The preparation variables are presented in Table 1.

2.2. Textural characterization and yield determination

The porous structure of all prepared and commercial activated carbons was analysed by N_2 adsorption-desorption at 77 K with a surface area analyser, ASAP 2010 Micromeritics. Nitrogen adsorption isotherms were measured at a relative pressure (P/P_0) range

Table 1. Preparation variables of activated carbons activated in a muffled furnace.

Product code	Raw material	Impregnated	Impregnation condition	
			Charge state	Contact time (h)
CPW-P-500	Coconut shell	30% H_3PO_4	Wet	02
PSW-P-500	Palm shell	30% H_3PO_4	Wet	02
PSW-P-ad-500	Palm shell	30% H_3PO_4	Semi-dried	02

from approximately 0.009–0.999. The Brunauer, Emmett and Teller (BET) equation was used to calculate the surface area and this equation was applied within the relative pressure range from 0.05 to 0.3 to determine the BET surface area. The single point total pore volume was measured from the amount of nitrogen adsorbed at the relative pressure of 0.99. The product yield was derived from the following equation.

$$\text{Yield}(\%) = \frac{W_2}{W_1} \times 100, \quad (11)$$

where W_1 and W_2 are weights of the precursor and activated carbon, respectively.

2.3. Adsorption studies

2.3.1. Test and standard metal ion solutions

Stock solution of $\text{Cu}(\text{II})$, 1000 mg L^{-1} , was prepared from copper(II) chloride dehydrate (Merck) using deionized distilled water (DDW). Stock solution of binary solute of $\text{Cu}(\text{II})$ and $\text{Ca}(\text{II})$ was prepared from a mixture of copper(II) chloride dehydrate (Merck) and calcium(II) nitrate tetrahydrate (GCE) while that of ternary solute of $\text{Cu}(\text{II})$, $\text{Ni}(\text{II})$ and $\text{Pb}(\text{II})$ were prepared from a mixture of copper (II) chloride dihydrate, nickel (II) nitrate hexahydrate (Fluka) and lead (II) nitrate (Riedel-deHaën) in such that the concentration of each solute was 1000 mg L^{-1} . Various concentrations of single (Cu), binary (Cu–Ca) and ternary (Cu–Ni–Pb) test solutions were prepared by subsequent dilution of the respective stock solution. The initial pH of the test solution was adjusted to the selected values using HNO_3 (65%, Merck) and NaOH (40.00 g mol^{-1} , Merck). All standard solutions were prepared from the proper dilution of the respective standard solution (1000 mg L^{-1}) using DDW acidified with 0.2% nitric acid.

2.3.2. Adsorption equilibria

All adsorption experiments were carried out in batches using 0.1 g various activated carbons added to 50 mL metal ion solution in a polypropylene tube. Shaking was applied in an orbital shaker at the rate of 160 revolutions per minute (rpm) and the equilibrium was attained by three days (37). Thereafter, the solutions were decanted and properly diluted using DDW acidified with 0.2% nitric acid prior to analysis by Perkin Elmer AAnalyst 400 flame atomic absorption spectrometry (FAAS). The concentration of metal ions in the solution before and after the adsorption was determined by FAAS. The following equation was used to calculate the metal uptake in mg by per unit mass of adsorbent

$$q = \frac{(C_0 - C_t)V}{1000m}, \quad (12)$$

where q = metal uptake mg g^{-1} -adsorbent; C_0 = initial concentration, mg L^{-1} ; C_t = concentration, at any time (t), mg L^{-1} ; V = volume of solution in a batch, mL; and m = mass of adsorbent used in a batch, g.

3. Results and discussion

3.1. FT-IR analysis (the functional group of activated carbon)

The effect of pyrolysis on the functional groups of activated carbon can be determined by Fourier-transform infrared spectroscopy (FT-IR). It is an important technique to determine the chemical properties of activated carbon. The spectrum bands obtained from activated carbon are given in Table 2. Pre-treatment was done to the carbon before the activation process. The observed spectrums of the activated carbon produced by chemical activation with 30% H_3PO_4 at different temperatures (500°C, 550°C and 600°C) are shown in Figures 1–3. Typical acidic functional groups such as phenols, carboxylic acids (or carboxylic anhydrides if they are close together) and carbonyl groups were presumed to be present in the surface functional groups

Table 2. List of functional group observed in the FTIR spectra of treated activated carbon at different temperatures PSW-P-500.

Functional groups	At 500°C	At 550°C	At 600°C
O–H stretching in phenol	3419.85 cm^{-1}	3426.14 cm^{-1}	3411.76 cm^{-1}
C=O stretching In carboxylic acid	1637.55 cm^{-1}	1637.13 cm^{-1}	1636.36 cm^{-1}

(44). In this study, the O–H stretching adsorption band was obtained at the range of 3411–3426 cm^{-1} . These peaks may be caused by water that is present in activated carbon. C=O stretching in carboxylic acid or C=N stretching in aliphatic amine spectrum absorption band were present at the range of 1636.36–1637.55 cm^{-1} . In different temperatures, remaining functional groups are the same in the produced activated carbon confirmed by FT-IR spectrums.

3.2. Evaluation of N_2 adsorption and porosity

The yield, BET surface area, average pore width and total pore volume of various activated carbons were obtained from the N_2 adsorption studies and are given in Table 3. It can be seen in Table 3 that the surface area of activated carbon produced with H_3PO_4 (1491 $\text{m}^2 \text{g}^{-1}$) is higher than that reported by the other researcher named Devarly Prahas who also used H_3PO_4 as a activating agent to produce the activated carbon. Terada and Miyoshi stated that “the surface area 849 $\text{m}^2 \text{g}^{-1}$ and 1081 $\text{m}^2 \text{g}^{-1}$ respectively”, which are lower than the surface area of produced activated carbon 1491 $\text{m}^2 \text{g}^{-1}$. Although, a study by Allwar et al. (45) shows that the surface area increased (1297 $\text{m}^2 \text{g}^{-1}$) when ZnCl_2 is used instead of H_3PO_4 as an activating agent; phosphoric acid is more preferred than zinc chloride due to the toxicological effects. Carbon activated with zinc chloride is not advisable for use in pharmaceuticals, water treatments and food industries to avoid contamination of the product (46). Zinc and chloride ions created problem of corrosion and inefficient chemical recovery is also associated with ZnCl_2 .

The surface area for palm oil shell is substantially greater than that for commercially activated carbon and coconut shell. From Table 3, it can also be seen that the higher pore volume (0.94 and 0.80 $\text{m}^3 \text{g}^{-1}$) palm shell oil wet and palm-oil semi-dried, respectively, were obtained from produced activated carbon than other researchers. The pore volume for commercially available activated carbon (0.67 $\text{m}^3 \text{g}^{-1}$) was higher than that for coconut (0.61 $\text{m}^3 \text{g}^{-1}$).

3.2.1. Adsorption from single-solute solution

Figure 4 shows the nonlinear Langmuir adsorption isotherms of Cu(II) for initial pH 3 and 5, by various activated carbons. Prepared activated carbons have very high affinity to bind Cu(II) as it is seen from the H-type shape in the isotherms according to the classification of Giles et al. (cited by (41)). The H-type shape also reveals complete adsorption in very low concentration. Linear Freundlich adsorption isotherms are depicted in Figure 5, followed by tabulation of the corresponding model parameters in Table 4.

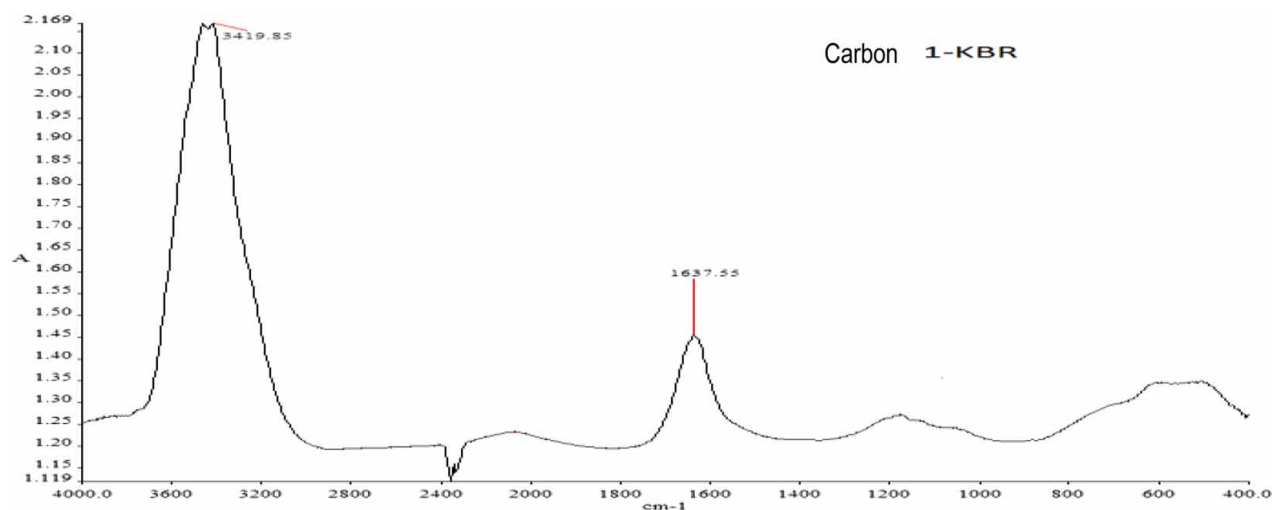


Figure 1. FTIR spectrum of treated activated carbon at 550°C in the absorbance mode.

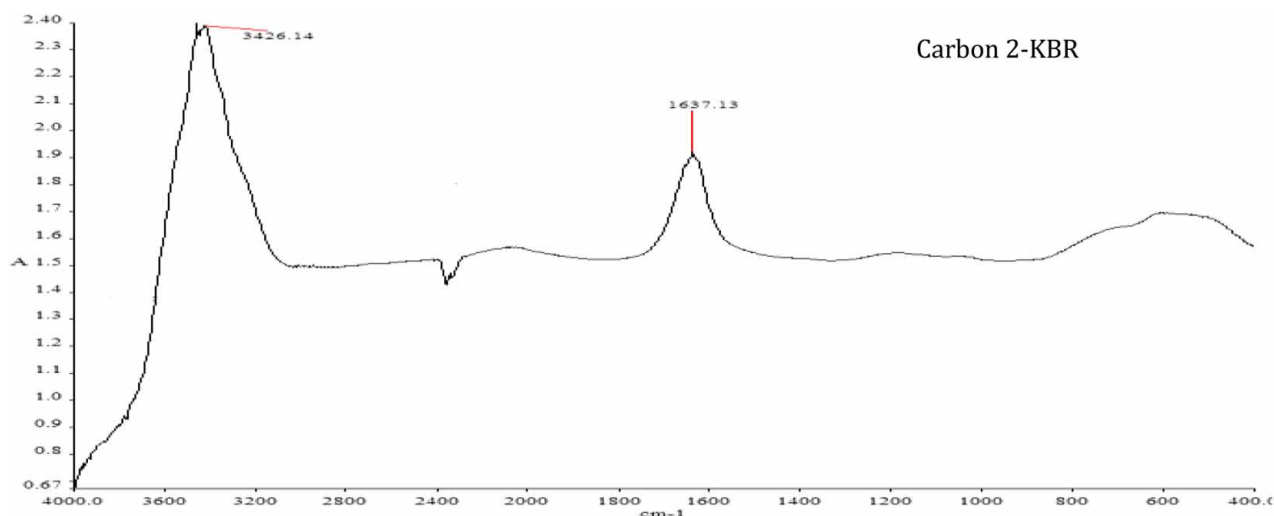


Figure 2. FTIR spectrum of treated activated carbon at 600°C in the absorbance mode.

The values of correlation coefficients of all Langmuir isotherms indicate that this model fits all the experimental data better than Freundlich throughout the experimental range of study. The three prepared activated carbons show almost similar q_{\max} (19–23 mg g⁻¹) which is 4–7 folds higher than that of commercial ones. The nonlinear Langmuir isotherm of Cu(II) by PSW-P-ad-500 steps more in low concentration which is an indication of its relatively stronger affinity towards Cu(II). That is, oil palm shell-derived activated carbon, PSW-P-ad-500, obtained from semi-dried feed-stock is the best scavenger for Cu(II), which is evident from its highest values of model parameters, namely q_{\max} , K_F and n , among experimental carbons. The oil palm shell-derived activated carbon had the highest adsorption capacity, due to its higher

surface area and also due to beneficial functional groups present on its surface.

3.2.2. The effect of pH

The removal of Cu(II) depends upon the nature and distribution of its hydroxo species in solution and their interaction with hydrous surface oxide (34, Panday et al., 1985), thus eventually depending on pH. The effect of pH on Cu(II) adsorption was observed from the constructed Langmuir (Figure 4) and Freundlich (Figure 5) isotherms for pH 3 and 5. With the increase in pH, at > 3 (pH_{ZPC}), the prepared activated carbon, through negatively charged sites, binds more positively charged species of copper by chemical and electrostatic interactions. In Figures 4 and 5, the curves for pH = 5 are slightly higher, indicating greater adsorption. At $\text{pH} \leq 3$, the protonated

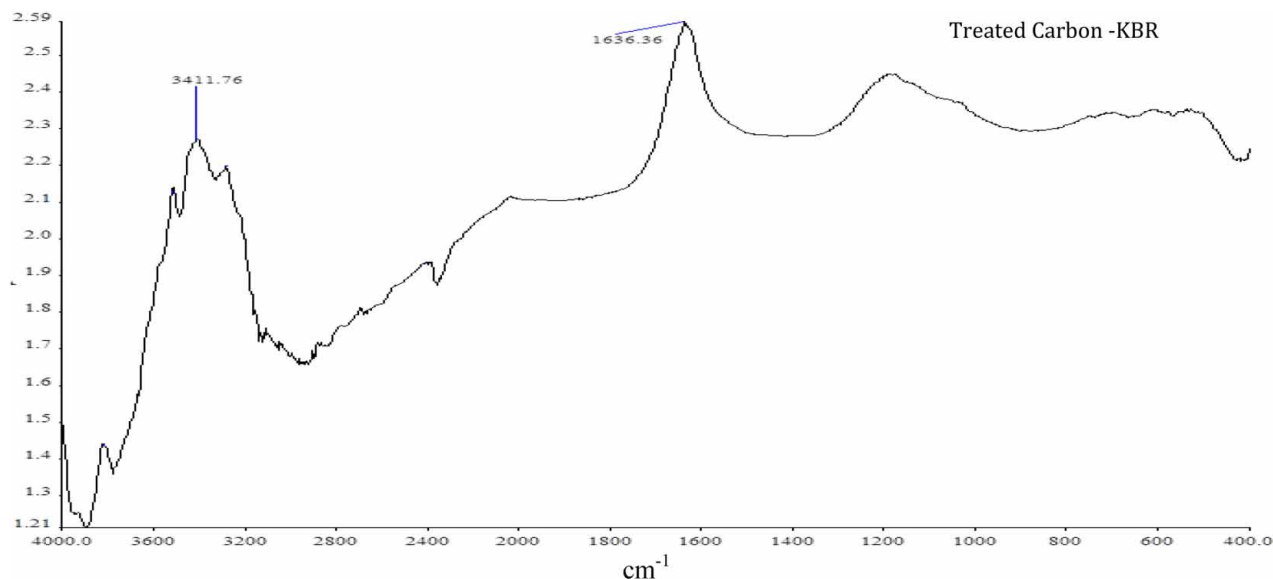


Figure 3. FTIR spectrum of treated activated carbon at 650°C in the absorbance mode.

Table 3. Yield, BET surface area, average pore width and total pores volume of various activated carbons.

Activated carbon	Yield %	S_{BET} $\text{m}^2 \text{g}^{-1\text{a}}$	Av pore width nm^{b}	V_{t} $\text{cm}^3 \text{g}^{-1\text{c}}$
CPW-P-500	44	1049	2.32	0.61
PSW-P-ad-500	46	1476	2.17	0.80
PSW-P-500	41	1491	2.52	0.94
CAC ^d	—	1320	2.04	0.67

^a S_{BET} = BET surface area.

^bAv = average.

^c V_{t} = total pore volume.

^dCAC = Aktivkohle (Riedel-deHaën).

surface sites of activated carbon exist mainly as neutral or positively charged species. Even at pH = 3, the moderately high adsorption capacity of the activated carbon implies the surface oxides function as ligands for metal ions while adsorption is attributed to inner-sphere complexation.

3.3. Competitive adsorption of Cu–Ca and evaluation of mechanism

Figure 6(a) and 6(b) shows the Langmuir isotherms of Cu(II) by the best selected scavenger for single (Cu), binary (Ca–Cu) and ternary (Cu–Ni–Pb) adsorption and Figure 6(c) shows linear Langmuir isotherm of Ca(II) for binary adsorption. The corresponding correlation coefficient of Langmuir isotherms of Cu(II) for binary solution is 0.99. The $q_{\text{max-binary}}$ of Cu(II) is obtained as 23.15 mg g^{-1} and the ratio of $q_{\text{max-binary}}$ to $q_{\text{max-single}}$ as 1.00, which means, according to

Equation (14), the adsorption of Cu(II) was not at all interfered by Ca(II).

The negative intercept of Ca(II) isotherm (see Figure 6(c)) indicates increasingly selective adsorption of Cu(II) over Ca(II). The q_{max} of Ca(II) was determined from the slope as only 1.17 mg g^{-1} . Because Ca(II) is a poor Lewis acid and Cu(II) being a transition metal ion exhibits fairly strong Lewis-acid characteristics, the very high selective adsorption of Cu(II) over Ca(II) illuminates the mechanism as inner-sphere complexation (47). Thus, the mechanism of bond formation of metal ions on carbon surface can be depicted as a result of major chemical, Lewis acid–base interaction, and minor electrostatic force of attraction (Figure 7). Here, each deprotonated surface functional group localizes electrons on surface and removes them from the π electron system of the basal planes. Thus providing a pair of donor electrons, each surface functional group functions as monodentate ligand, Lewis base, while the adsorbent as a whole is a polydentate ligand. Corapcioglu and Huang (34) reported the sorption of a number of heavy metal ions on activated carbon as surface complexation either through inner-sphere or outer-sphere complexation. Therefore it could be concluded that the adsorption of Cu(II) on acid activated carbon was resulted from the chemisorption rather than the physical adsorption.

3.4. Competitive adsorption of Cu–Ni–Pb

The interaction of metallic species with living systems and adsorbents can be demonstrated by the properties of metal ions as Lewis acids (48). Thus the classification of metals by their Lewis acidity would be

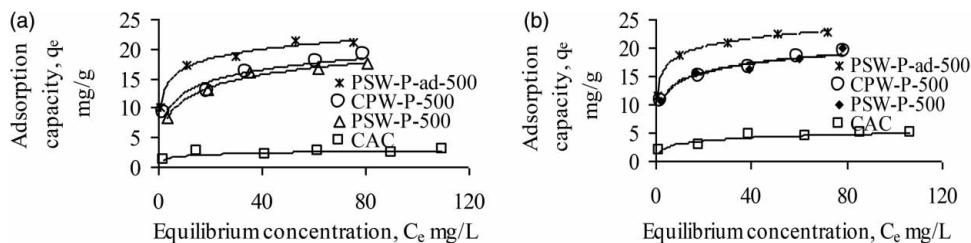


Figure 4. Langmuir adsorption isotherms of Cu(II) at initial pH 3 (A) and pH 5 (B) by various activated carbons while initial concentrations were varied, from <0 to <120 mg L^{-1} .

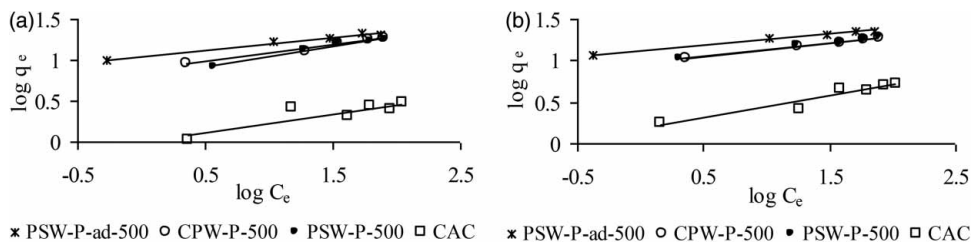


Figure 5. Freundlich adsorption isotherms of Cu(II) at pH 3 (A) and at pH 5 (B) while initial concentrations were varied, from <-0.5 to <2.5 mg L^{-1} .

Table 4. Langmuir and Freundlich parameters for the adsorption of Cu(II) in the single-solute solution.

Activated carbon code	pH	Langmuir parameters				Freundlich parameters		
		q_{\max} mg g^{-1}	b L mg^{-1}	K_L L g^{-1a}	r^2	K_F mg g^{-1}	n L mg^{-1}	r^2
PSW-P-ad-500	3	21.23	0.55	11.68	0.997	11.25	6.51	0.976
CPW-P-500	3	19.57	0.16	3.13	0.991	7.54	4.89	0.977
PSW-P-500	3	18.62	0.17	3.16	0.997	6.35	4.15	0.972
CAC	3	2.91	0.15	0.43	0.967	1.02	4.45	0.748
PSW-P-ad-500	5	23.09	0.59	13.53	0.999	13.16	7.38	0.989
CPW-P-500	5	19.76	0.22	4.40	0.995	9.21	6.00	0.997
PSW-P-500	5	19.46	0.23	5.40	0.989	9.64	6.42	0.976
CAC	5	5.56	0.09	0.50	0.976	1.50	3.75	0.928

^a $K_L = q_{\max} \times b = \text{Langmuir equilibrium constant.}$

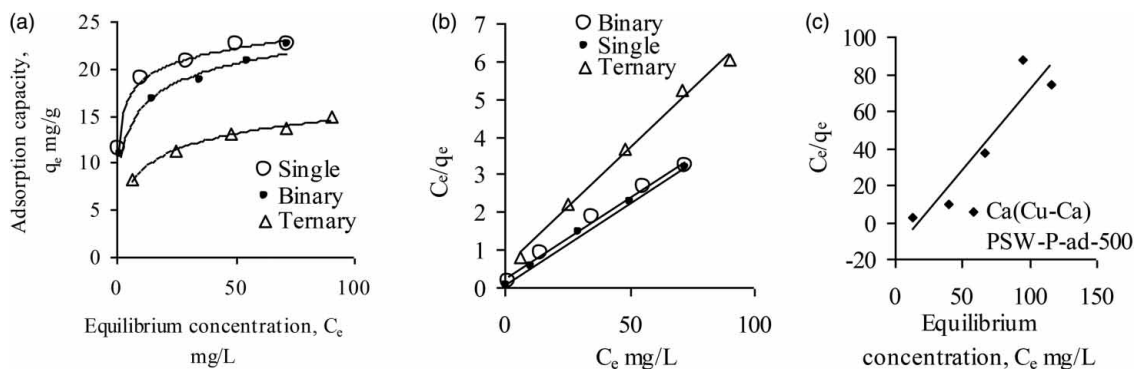


Figure 6. Langmuir isotherms of Cu(II) (a, b) and Ca(II) (c) while Cu(II) adsorptions were conducted from single (Cu), binary (Ca–Cu) and ternary (Cu–Ni–Pb) solutions and Ca(II) was adsorbed in binary solution (Ca–Cu) by PSW-P-ad-500 at initial pH 5 varying initial concentrations, from <0 to <100 mg L^{-1} .

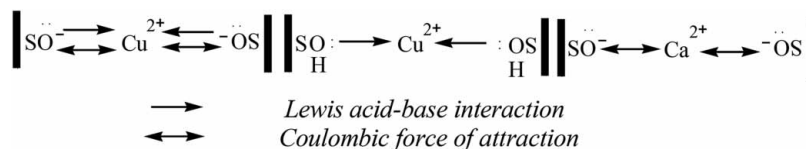


Figure 7. The proposed interactions of Cu(II) and Ca(II) ions onto the surfaces of activated carbon.

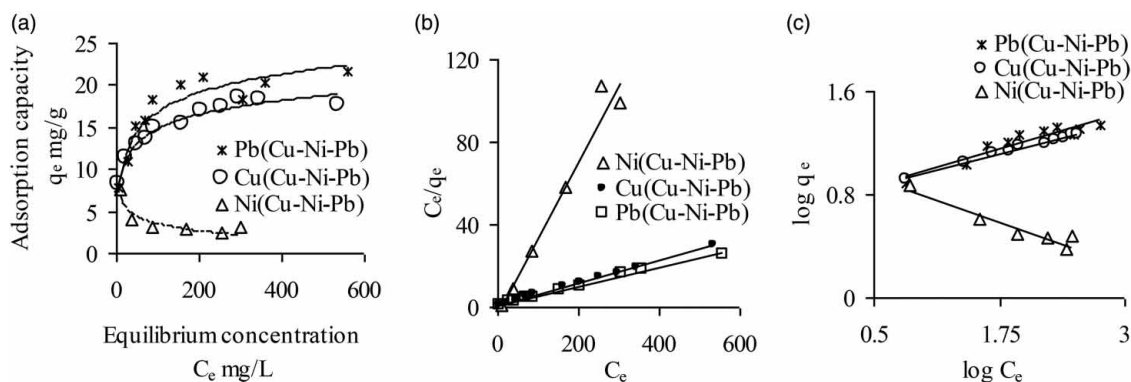


Figure 8. Langmuir nonlinear (a), linear (b) and Freundlich (c) isotherms of ternary solute, Cu(II), Ni(II) and Pb(II), by PSW-Pad-500 at initial pH 5 while their initial concentrations were varied, from <0 to $\leq 600 \text{ mg L}^{-1}$. (Ni samples were analysed for the concentration range up to 305 mg L^{-1}).

Table 5. Model parameters for the adsorption isotherms of Ni(II), Pb(II) in ternary and Cu(II) in single and ternary solutes solution at pH 5.

Metal ions mg L^{-1}	Langmuir parameters				Freundlich parameters		
	$q_{\text{max}} \text{ mg g}^{-1} (\text{mmol g}^{-1})$	$b \text{ L g}^{-1}$	$K_L \text{ mg L}^{-1}$	r^2	$K_F \text{ mg g}^{-1}$	$n \text{ L g}^{-1}$	r^2
Ni^{2+} -ternary-<25-<600	2.68 (0.046)	-0.127	-0.340	0.968	11.68	-3.70	0.904
Pb^{2+} -ternary-<25-<600	21.74 (0.105)	0.048	1.044	0.993	5.70	4.40	0.875
Cu^{2+} -ternary-<25-<600	18.66 (0.294)	0.054	1.008	0.997	5.87	5.04	0.988
Cu^{2+} -ternary-<25-<120	15.85 (0.249)	0.120	1.902	0.993	5.50	4.55	0.994

consistent in their remediation approach. This type of classification divided metals into three groups based on their observed affinity for different ligands as Class (a) “hard metals”, Class (b) “soft metals” or Class (c) borderline “difficult to distinguish as hard or soft” (31). The competitive effect among borderline and soft cations was studied from the adsorption in a solution containing ternary solute of Cu(II), Ni(II) and Pb (II). Figure 8 shows the Langmuir (a and b) and Freundlich (c) adsorption isotherms of Cu(II), Ni(II) and Pb (II) while their initial concentrations were varied in the ternary solution from <25 to $\leq 600 \text{ mg L}^{-1}$ and the initial pH was kept constant at 5. Since single Cu(II) adsorption was conducted with varying initial concentrations from <5 to $<120 \text{ mg L}^{-1}$ and no detectable residual concentration was found by prepared activated carbons for the initial concentration of 5 mg L^{-1} , the effect of competing ions was also studied by

constructing Langmuir isotherms for the same concentration range mentioned in Figure 6(a) and 6(b). The model parameters of these isotherms are presented in Table 5. r^2 values are generally higher for the Langmuir curve-fit.

The favourable adsorptions of Cu(II) and Pb(II) are realized from the considerably high q_{max} and the higher values of “ n ” (Table 5). The total adsorption capacities of multi solute in ternary solution ($0.445 \text{ mmol g}^{-1}$) exceed that of single solute ($23.09 \text{ mg g}^{-1} = 0.36 \text{ mmol g}^{-1}$). The HSAB concept is an initialism for “hard and soft Lewis acid and bases” (47). Also known as the Pearson acid–base concept (49), HSAB is widely used in chemistry for explaining stability of compounds, reaction mechanisms and pathways. This finding is in accordance with the concept of HSAB that soft Lewis base, basal structural unit (soft site) of carbon prefers soft Lewis acid, Pb(II)

while harder site (surface oxide group) prefers relatively harder ion, Cu(II). But the presence of Cu(II) impeded the adsorption of softer Pb(II) largely (the ratio of $q_{\text{max-ternary}}$ to $q_{\text{max-single}}$ is 0.34), indicating that Pb(II) is marginally soft ion and that it adsorbed predominantly onto the surfaces. Adsorption is suppressed by the presence of other ions.

The interference of Pb(II) and Ni(II) on Cu(II) adsorption is little as the ratio of $q_{\text{max-ternary}}$ (conc. range <25 to <120 mg L⁻¹) to $q_{\text{max-single}}$ has the

value 0.69. With the increase in initial concentrations of Cu(II), the ratio $q_{\text{max-ternary}}$ (conc. range <25 to ~600 mg L⁻¹) to $q_{\text{max-single}}$ increases to 0.80 as the affinity increases towards Cu(II). A gradual runaway in the adsorption capacity of Ni(II) with the increase in equilibrium concentration indicates the selective adsorption of Cu(II) over Ni(II). This finding is in agreement with Irving-Williams order (cited by Shriver et al. (50)), which describes the stability of inner-sphere complexes of transition metal cations as: $\text{Mn}^{2+} < \text{Fe}^{2+} < \text{Co}^{2+} < \text{Ni}^{2+} < \text{Cu}^{2+} > \text{Zn}^{2+}$. The adsorption selectivity order can be expressed in series as: $\text{Pb(II)} > \text{Cu(II)} \gg \text{Ni(II)}$. The comparison in q_{max} was made in the unit of mmol g⁻¹ instead of mg g⁻¹.

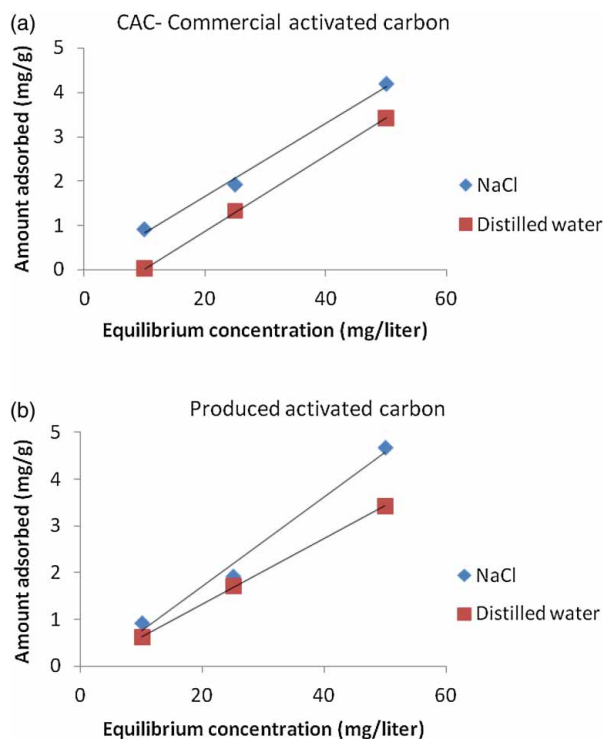


Figure 9. (a) Adsorption isotherm of paraquat onto commercial activated carbon (^dCAC) at 25°C in NaCl (0.9%) solution and distilled water. (b) Adsorption isotherm of paraquat onto produced activated carbon (PSW-P-500) at 25°C in NaCl (0.9%) solution and in distilled water.

3.5. Adsorption isotherm of paraquat as a toxin onto activated carbon

The adsorption isotherms of paraquat in different solvents at 25°C both onto the commercial activated carbon and the produced activated carbon are shown in Figure 9(a, b). The logarithm of the amount adsorbed was plotted linearly against the logarithm of equilibrium concentration. For both activated carbons, the amount of paraquat adsorbed was in the following order:

In NaCl solution (physiological saline solution) > in distilled water.

From Table 6, it can be seen that the amount of paraquat adsorbed is more in NaCl solution (saline solution) than in distilled water. Moreover, in both solvents, the produced activated carbon adsorbed larger amount of paraquat compared to the commercial activated carbon. Generally, anion is specifically adsorbed onto activated carbon in respect to saline adsorption. On the surface of activated carbon an electrical double layer is also formed, which attracts cation in solution (51). In the liquid phase, paraquat dichloride as a salt dissociates into paraquat cation and chloride anion. It was recommended that the surface of

Table 6. A comparison onto commercial activated carbon (^dCAC) and produced activated carbon (PSW-P-500) amount of adsorbed paraquat (PQ).

Name of carbon	Characteristics		Types of solvent	Amount adsorb (mg g ⁻¹)		
	Surface area (m ² g ⁻¹)	Total pore volume (cm ³ g ⁻¹)		At 10 mg L ⁻¹	At 25 mg L ⁻¹	At 50 mg L ⁻¹
Commercial activated carbon (CAC)	1320	0.67	H ₂ O	0.02	1.32	3.42
			NaCl (0.9%) solution	0.92	1.72	4.18
Produced activated carbon (PSW-P-500)	1491	0.94	H ₂ O	0.62	1.72	3.62
			NaCl (0.9%) solution	0.92	1.92	4.68

activated carbon attracts chloride anion followed by the adsorption of the paraquat cation. However, due to the electrical repulsive force between the surface oxygen groups and chloride anion, the surface oxygen groups inhibit the approach of chloride anion onto the surface of the adsorbent. The resulting electrical interaction between the surface charge of the adsorbent and paraquat cation might be the cause of enhancing effect of salts to paraquat adsorption by activated carbon *in vitro*. In this study, the adsorption capacity of activated carbon, both commercial and that produced was observed to be better in case of sodium chloride solution.

Here, it was assumed that the reason for the higher adsorption capacity for paraquat onto activated carbon in NaCl (0.9%) solution was as follows:

1. In solution the dissociation of paraquat was inhibited by sodium chloride, so the phenomenon of salting out occurred in solution, and consequently paraquat was adsorbed more abundantly onto the activated carbon.
2. As the properties of adsorbents dominated paraquat removal, there is a correlation between the properties of activated carbon and the adsorption characteristics of paraquat.

4. Conclusion

- (i) Phosphoric acid activation in the presence of controlled air (by the design default of furnace) produces activated carbon suitable for removing borderline and soft metal ions. Although the commercial activated carbon has identical surface area, its Cu(II) removal capacity is very low. That is, rather than porosity, surface functional groups are the major factor in removing metal ions.
- (ii) Adsorption capacity of Cu(II) by one of the palm shell-derived activated carbons, PSW-P-500, is higher than that of the coconut shell-derived carbon, CPW-P-500 and PSW-P-ad-500, although both activated carbons have similar BET surface area. This might be due to the variations in precursor type and/or in pre-treatment.
- (iii) The inner-sphere surface-metal complexation is speculated as predominant adsorption mechanism while Cu(II) or borderline metal ions are expected to be adsorbed preferentially, on H₃PO₄ acid activated carbon, over alkali and alkaline earth metals.
- (iv) The effect of Pb(II) and Ni(II) on the adsorption of Cu(II) is a little suppressive. The

selectivity order in the adsorption of Cu(II), Ni(II) and Pb(II) can be expressed as Pb(II) > Cu(II) \gg Ni(II).

- (v) The high adsorbing capacity of activated carbon, both commercial and produced was evaluated by the *in vitro* test of carbon as an adsorbent of toxin (paraquat) in this study. So, it was concluded that both commercial and produced activated carbon were effective to promote adsorption removal of paraquat and NaCl (0.9%) solution is the most effective solvent. Paraquat was found to be adsorbed more by the produced activated carbon.

Acknowledgements

We thank the Department of Chemistry, UTM Johor Bahru for financial support through Intensification of Research in Priority Areas [vote no. 74029], and thankful to the Research Management Center, IIUM, and financial support through research grants "Endowment type B" and "Fundamental Research Grant Scheme grants".

Disclosure statement

No potential conflict of interest was reported by the authors.

References

1. Smith, Eugene, W.; Smith, Aileen M. *Life*. **1972**, 2, 74–79.
2. Cech, T.V. *Principles of Water Resources History, Development, Management, and Policy*, 2 ed.; John Wiley & Sons, Inc.: River Street, Hoboken, NJ, **2005**; p. 120.
3. <http://water.epa.gov/polwaste/nps/whatis.cfm>.
4. Strelko, V. Jr.; Malik, D.J. *J. Colloid Interface Sci.* **2002**, 250, 213–220.
5. Inagaki, M. *New Carbon Mater.* **2009**, 24 (3), 193–232.
6. Patel, M.A.; Ou, M.S.; Harbrucker, R.; Aldrich, H.C.; Busko, M.L.; Ingram, L.O.; Shanmugam, K.T. *Appl. Environ. Microbiol.* **2006**, 72 (5), 3228–3235.
7. Palonen, H.; Tjerneld, F.; Zacchi, G.; Tenkanen, M. *J. Biotechnol.* **2004**, 107 (1), 65–72.
8. Laini, J.; Calafat, A. *Carbon*. **1991**, 29 (6), 949–953.
9. Wigmans, T. *Carbon*. **1989**, 27 (1), 13–22.
10. Girgis, B.S.; Khalil, L.B.; Tawfik, T.A.M. *J. Chem. Tech. Biotechnol.* **1994**, 61, 87–92.
11. Caturla, F.; Molina, M.S.; Reinoso, F.R. *Carbon*. **1991**, 29 (10), 999–1007.
12. Edberg S.; Rice, E.W.; Karlin, R.J.; Allen, M.J. *J. Appl. Microbiol.* **2000**, 88, 1068–1168.
13. Toles, C.A.; Marshall, W.E. *Sep. Sci. Technol.* **2002**, 37, 2369–2383.
14. Dastgheib, S.A.; Rockstraw, D.A. *Carbon*. **2001**, 39, 1849–1855.

15. Rahman, R.A.; Surif, S. Metal Finishing Wastewater: Characteristics and Minimization. In *Waste Management in Malaysia: Current Status and Prospects for Bioremediation*. Ministry of Science, Technology and the Environment, Malaysia. 1993; pp 3–7.
16. Das, K.K.; Das, S.N.; Dhundasi, S.A. *Indian J. Med Res.* **2008**, *128* (4), 412–425.
17. Ministry of Health. Annual Report. Malaysia: Ministry of Health Malaysia, 1997.
18. Ministry of Health. Annual Report. Malaysia: Ministry of Health Malaysia, 1999.
19. Ukai, S.; Kawase, S. *Jpn. J. Toxicol. Environ. Health.* **1985**, *31*, 283–297.
20. Mascie-Taylor, B.H.; Thompson, J.; Davison, A.M. *Lancet*, **1983**, *321*, 1376–1377.
21. Smith, L.L.; Wright, A.; Wyatt, I. *Br. Med. J.* **1974**, *4*, 569–571.
22. Nokata, M.; Tanaka, T.; Tsuchiya, K.; Yamashita, M. *Acta Pharmacol. Toxicol.* **1984**, *55*, 158–166.
23. Staiff, D.C.; Irle, G.K.; Felsenstein, W.C. *Bull. Environ. Contam. Toxicol.* **1973**, *10*, 193–197.
24. Yamashita, M.; Naito, H.; Takagi, S. *Hum. Toxicol.* **1987**, *6* (1), 89–90.
25. Neuvonen, P.J. *Clin. Pharmacokinet.* **1982**, *7*, 465–489.
26. Neuvonen, P.J.; Olkkola, K.T. *Med. Toxicol.* **1988**, *3*, 33–58.
27. Palatnick, W.; Tenenbein, M. *Drug Safety.* **1992**, *7*, 3–7.
28. Nakamura, M.; Tanada, S.; Nakamura, T.; Keshi, H.; Kawanishi, T. *Chem. Express.* **1989**, *4*, 357–360.
29. Kitakouji, M.; Miyoshi, T.; Tanada, S.; Nakamura, T. *Bull. Environ. Contam. Toxicol.* **1989**, *42*, 926–930.
30. Alfara, A.; Frackowiak, E.; Béguin, F. *Appl. Surf. Sci.* **2004**, *228*, 84–92.
31. Ahrland, S.; Chatt, J.; Davies, N.R. *Q. Rev. Chem. Soc.* **1958**, *12*, 265–276.
32. IUPAC Technical Report. Published by Duffus J.H. “Heavy Metals” – A Meaningless Term? *Pure Appl. Chem.* **2002**, *74*, 793–807.
33. Faust, S.D.; Aly, O.M. *Adsorption Processes for Water Treatment*; Butterworth Publishers: Stoneham, **1987**; pp 16–20.
34. Corapcioglu, M.O.; Huang, C.P. *Water Res.* **1987**, *21*, 1031–1044.
35. Reed, B.E.; Vaughan, R.; Jiang, L. *J. Environ. Eng.* **2000**, *126*, 869–873.
36. Reed, B.E.; Matsumoto, M.R. *Carbon.* **1991**, *29*, 1191–1201.
37. Arup, K.S.G. *Environmental Separation of Heavy Metals: Engineering Processes. Technology and Engineering*, CRC Press, Florida, **2001**, pp. 2007.
38. Mohan, D.; Singh, K.P. *Water Res.* **2002**, *36*, 2304–2318.
39. Mohan, D.; Chander, S. *Colloid. Surf. A.* **2001**, *177*, 183–196.
40. Rahman, M.; Awang, B.S.; Mohosina, B.Y.; Kamaruzzaman, W.B.; Nik, W.; Adnan, C.M.C. *APCBEEES Procedia.* **2012**, *2* (1), 297–302.
41. Jankowska, H.; Swiatkowski, A.; Choma, J. *Active Carbon*; Ellis Horwood Limited: West Sussex, **1991**, pp 177–178.
42. Guo, J.; Lua, A.C. *Micropor. Mesopor. Mater.* **1999**, *32*, 111–117.
43. Scott, W.W. *Standard Methods of Chemical Analysis: A Manual of Analytical Methods and General Reference for the Analytical Chemist and Advance Student*, 2nd ed., **1917**, D. Van Nostrand, New York.
44. Boehm, H.P. *Carbon.* **1994**, *32* (5), 759–769.
45. Allwar, A.B.M.N.; Asri, M.B.M.N. *J. Phys. Sci.* **2008**, *19* (2), 93–104.
46. Srinivaskannan, C.; Bakar, M.Z.A. *Biomass Bioenergy.* **2004**, *27*, 89–96.
47. Vogels, A.I. *Text Book of Quantitative Chemical Analysis*, 5 ed.; John Wiley & Sons, Inc., New York, **1989**.
48. Haas, K.L.; Franz, K.J. *Chem. Rev.* **2009**, *109* (10), 4921–4960.
49. Pearson, R.G. *J. Chem. Edu.* **1968**, *45*, 581–587.
50. Shriver, D.F.; Atkins, P.W.; Langford, C.H. *Inorganic Chemistry*; Oxford University Press: Walton Street, Oxford, **1991**; pp. 222.
51. Urano, K.; Sonai, M.; Nakayama, R.; Kobayashi, Y. *Nippon Kagaku Kaishi (in Japanese).* **1976**, *11*, 1773–1782.